Thomas's double binary-encounter integrals. Explicit verification of this possibility would considerably elucidate the theoretical foundation of Gryzinski's prescriptions for predicting charge-transfer cross sections.

In much of this paper we have criticized Gryzinski's prescriptions, on both formal and pragmatic grounds. Gryzinski's prescriptions do have one very important practical virtue, however: Compared with most other theories, Gryzinski cross sections—in their original form or modified as suggested in Sec. IV—are very easy to compute. It is interesting, therefore, that at high energies, using Eq. (5), Gryzinski predicts

$$\frac{\sigma_{10}E^3\lambda^3}{U_B} = \frac{2\pi e^4}{3}\frac{\lambda^2 E^2}{U_A^2}\left[\frac{7+3\lambda E/U_A}{(\lambda E/U_A+1)^3}\right] = F\left(\frac{\lambda E}{U_A}\right). \quad (17)$$

Equation (17), which asserts $\sigma_{10}E^3\lambda^3/U_B$ is a function of $\lambda E/U_A$, is surprisingly close to the scaling law inferred by Bates and Mapleton[5] from their modification of the Thomas theory. Therefore, in the spirit of their paper, in Fig. 10, we have plotted the experimental values of $\sigma_{10}E^3\lambda^3$ against $\lambda E/U_A$, for the noble gases and potassium from Figs. 1–6. (We have multiplied the values for He and K by 3 and 6, respectively, to obtain six equivalent electrons in each case.) It can be seen that the heavy noble gases scale exceptionally well; however, all points lie close together in the region $10^{-1}<\lambda E/U_A<10$. The fact that potassium agrees so well with a curve obtained from scaling only noble-gas data may be construed to mean that this curve can be used for predicting other charge-transfer reactions in this range of values of $\lambda E/U_A$.

Alignment of the H₂⁺ Molecular Ion by Selective Photodissociation. II. Experiments on the Radio-Frequency Spectrum*

C. B. Richardson,† K. B. Jefferts,‡ and H. G. Dehmelt
Department of Physics, University of Washington, Seattle, Washington
(Received 10 August 1967)

Magnetic resonance transitions have been observed among several Zeeman sublevels of the hyperfine states of H₂⁺ in magnetic fields from 50 to 115 mG. The following g-factor ratios $g(KF_2F)/g(K'F_2'F')$ have been determined: $g(1\ \frac{1}{2}\ \frac{3}{2})/g(1\ \frac{1}{2}\ \frac{1}{2})=0.584(3)$; $g(1\ \frac{3}{2}\ \frac{3}{2})/g(1\ \frac{3}{2}\ \frac{5}{2})=1.241(6)$; $g(1\ \frac{1}{2}\ \frac{3}{2})/g(3\ \frac{3}{2}\ \frac{3}{2})=1.051(5)$. An analysis using the ratios yields equations relating the hyperfine interaction constants b, c, and d in the Hamiltonian $H=b\mathbf{I}\cdot\mathbf{S}+c I_z S_z+d\mathbf{K}\cdot\mathbf{S}$, such as $(\sqrt{2}c/6-\sqrt{2}d/3)/(3b/2+23c/30-d/6)=(8/\sqrt{5})\{[g(1\ \frac{1}{2}\ \frac{3}{2})/g(3\ \frac{3}{2}\ \frac{3}{2})]-1\}$. When nuclear contributions to the g factors are included and a weighted average of the measured ratios is used with theoretical values of b and c from the literature, a value for d may be obtained. The result is $d=32.2\pm5.1$ MHz. With this it is possible to predict the H₂⁺ hfs spectrum in the 20-cm region with an error estimate of a few MHz. $(1\ \frac{3}{2}\ \frac{3}{2})-(1\ \frac{1}{2}\ \frac{3}{2})=1415.3$ MHz; $(1\ \frac{3}{2}\ \frac{3}{2})-(1\ \frac{1}{2}\ \frac{1}{2})=1400.9$ MHz; $(1\ \frac{3}{2}\ \frac{5}{2})-(1\ \frac{1}{2}\ \frac{3}{2})=1398.1$ MHz; $(1\ \frac{3}{2}\ \frac{1}{2})-(1\ \frac{1}{2}\ \frac{3}{2})=1322.4$ MHz; $(1\ \frac{3}{2}\ \frac{1}{2})-(1\ \frac{1}{2}\ \frac{1}{2})=1308.2$ MHz. The ion sample is contained electrically in an rf quadrupole trap where production and analysis of alignment is by selective optical excitation by linearly polarized light of the transition $1s\sigma$-$2p\sigma$ leading to dissociation. The mechanism is briefly reviewed. A description is given of the trap and apparatus for the detection of the trapped ions and magnetic resonance.

INTRODUCTION

IN an earlier paper,[1] herein called I, a discussion was presented of the feasibility of alignment of a sample of free hydrogen molecule ions by optical means to permit observation of the rf spectrum of this simplest of all molecules. The source of the level splittings are the several magnetic interactions in the ion which depend differently on the average positions of the electron and protons, so that a measurement of the spectrum provides a very exacting test of the ground-state molecular

wave function, which is believed known to very high precision.[2] Interesting small effects such as unknown electron-proton radiative corrections, centrifugal stretching, vibrational effects, rotational mixing of excited states,[3] and electron slippage should be revealed. Further, H₂⁺ has been discussed as a possible interstellar radio source.[4] A laboratory measurement of the spectrum would aid in a search for this radiation.

The method discussed in I for detection of magnetic resonance in H₂⁺ is akin to the optical-pumping method

[1] H. G. Dehmelt, K. B. Jefferts, Phys. Rev. 125, 1318 (1962).

[2] D. R. Bates, K. Ledsham, A. L. Stewart, Phil. Trans. Roy. Soc. London, Ser. A 246, 215 (1953).

[3] J. H. Van Vleck, Phys. Rev. 33, 467 (1929).

[4] K. S. Stankevich, Astron. Zh. 37, 983 (1960) [English transl.: Soviet Astron.—AJ 4, 917 (1961)]; D. R. Bates, Monthly Notices Roy. Astron. Soc. 111, 303 (1951); G. B. Field, W. B. Sommerville, and K. Dressler, Ann. Rev. Astron. Astrophys. 4, 207 (1966).

widely used for atoms but not applied to molecules. It may also be viewed as related to Bloch and Alvarez's experiment[5] on the magnetic moment of the neutron. This was the first instance in which collisional orientation, by means of the magnetic interaction between neutron and ferromagnetic polarized atoms, was used in rf spectroscopy. Other members of this group of collisional-orientation schemes, besides the already mentioned optical-pumping schemes, are electron impact and electron exchange,[6] also taking the form of metastability[7] and charge exchange.[8] Of these, electron exchange has recently served in an experiment based on the ion storage-collison technique like the present one to observe the $^3He^+$ hfs spectrum at very high resolution.[9]

The cross section for optical excitation of the molecule from the ground state $1s\sigma$ to the first excited state $2p\sigma$ depends on the magnetic substate of the ion when the exciting light is polarized. Because the excited state is repulsive, the ion has a negligibly small probability of radiative return to the ground state before dissociation occurs. Detailed calculations in I for the rotational states $K=0$, 1, 2 showed an approximate threefold variation in photodissociation cross section among the 30 magnetic substates $|F,M\rangle$ when the light is linearly polarized in the direction of a weak applied magnetic field.

An experiment was proposed in which the ions were to be created by pulsed electron bombardment, and electrodynamically trapped[10] in a region of intense light flux. Accompanying the decrease in the number trapped as photodissociation destroys the $H_2{}^+$ would be an increasing alignment in those remaining. Excitation of an rf magnetic-dipole transition between substates $|F,M\rangle$ with different photodissociation cross sections would increase the ion decay rate and thereby become detectable. Work of others[11] showed that with commercially available light sources photodissociation times as short as 0.1 sec were possible. Disalignment by collision and loss of ions from the trap were expected to be at a slower rate at pressures attainable in a baked system evacuated by sputter-ion pumping.

An experiment to demonstrate alignment was undertaken and proved successful.[12] In this paper we wish to report more fully on this and subsequent experiments.[13]

[5] L. W. Alvarez, F. Bloch, Phys. Rev. **67**, 111 (1940).
[6] H. G. Dehmelt, Phys. Rev. **109**, 381 (1958); **103**, 1125 (1956).
[7] F. D. Colegrove, L. D. Shearer, and G. K. Walters, Phys. Rev. **132**, 2561 (1963).
[8] H. G. Dehmelt and F. G. Major, Phys. Rev. Letters **8**, 213 (1962).
[9] E. N. Fortson, F. G. Major, and H. G. Dehmelt, Phys. Rev. Letters **16**, 221 (1966).
[10] W. Paul, O. Osberghaus, and E. Fischer, Forschungsber. Wirtsch. Verkehrsministeriums Nordrhein-Westfalen **415** (1958); E. Fischer, Z. Physik **156**, 1 (1959); R. F. Wuerker, H. Shelton, and R. V. Langmuir, J. Appl. Phys. **30**, 342 (1958).
[11] W. Linlor, C. F. Barnett, and R. Reinhardt, University of California Radiation Laboratory Report No. UCRL 4917, 1957 (unpublished).
[12] K. B. Jefferts, thesis, University of Washington, 1962

ION TRAPPING

In measurements of the magnetic splitting of ground states of free atomic and molecular ions by magnetic resonance, advantage may be taken of the particle's charge to extend the interaction time with a suitably applied perturbation and thereby possibly achieve a significant improvement in precision.[14] This extension may be accomplished by holding the ions in an rf trap of the type described by Paul et al., and Wuerker et al.[10] About 40 collisions with the parent background gas are required on the average to cause a trapped ion to leave the trap, so that interaction times of 1 sec or longer may be obtained with common high-vacuum techniques.

It is further necessary for the phase memory of the internal precessions to persist for the interaction time. Elastic collisions introduce random phase shifts, but these should be negligible.[15] For ions with nonspherical charge distributions, such as $H_2{}^+$, collisions may cause ΔM transitions, termintating the phase memory. The vacuum requirements for high resolution are therefore greater for these ions. If the splitting has a first-order Zeeman effect, the requirements for field homogeneity and stability will in general be severe. These requirements are relaxed for field-independent transitions.

It was possible to meet the conditions for high resolution for the $|10\rangle \leftrightarrow |00\rangle$ hyperfine transition in $^3He^+$ at 8666 MHz which has recently been detected with a linewidth of 10 Hz.[9]

Excellent descriptions of ion trapping have been given in the original papers.[10] We will review the mechanism briefly for convenience.

The three-dimensional containment of ions is effected by an electric field in which the particle experiences a force of strength proportional to its displacement from the center of symmetry. The proper field is derived from a potential of cylindrical symmetry of the form

$$\phi = \phi_0 \cos\Omega t[\tfrac{1}{2}(z^2-r^2)/z_0{}^2], \qquad (1)$$

resulting from application of a cosineusoidal emf of frequency Ω between an hyperbolic electrode of the form $r^2 = 2(z^2+r_0{}^2)$ and a pair of the form $r^2 = 2(z^2-z_0{}^2)$. A necessary condition for the containment of an ion of specific change e/m created in the electric field is

$$\Omega > 1.484[2e\phi_0/mz_0{}^2]^{1/2}. \qquad (2)$$

An ion created from a neutral particle with thermal velocity, if trapped, moves in a symmetric orbit passing through the trap center. The exact expression for the orbit is complicated, but for the case of Ω well above

(unpublished); K. B. Jefferts, H. G. Dehmelt, Bull. Am. Phys. Soc. **7**, 432 (1962).
[13] Early results of these experiments were reported at the Topical Conference on The Physics of Free Atoms, Berkeley September, 1966 (unpublished).
[14] H. G. Dehmelt, Advances in Atomic and Molecular Physics, Vol. III (to be published).
[15] R. H. Lambert and F. M. Pipkin, Phys. Rev. **129**, 1233 (1963); S. B. Crampton, D. Kleppner, and N. F. Ramsey, Phys. Rev. Letters **11**, 338 (1963).

threshold it is well approximated as harmonic "macro-motion" with frequency $\omega_z = 2\omega_r = \sqrt{2e\phi_0/mz_0^2\Omega}$, on which a small amplitude "micromotion" with a spectrum $n\Omega$, $n = 1, 2, \cdots$ is superimposed. In this approximation, the depth of the harmonic well in the z direction is $eD_z = e\phi\omega_z/\sqrt{2}\Omega$, and in the r direction is $eD_r = eD_z r_0^2/4z_0^2$. We note from these expressions that if the condition for trapping is satisfied and Ω is then decreased to approach threshold, ω_z and D_z increase. Accompanying the increase in D_z is an increase in the maximum amplitude of the micromotion. Hence, an ion which is formed at a particular point in the trap is apparently more tightly bound nearer threshold but probably has a larger orbit (the orbit size depends on the phase ϕ at formation). It has been shown[10] that the probability that an ion takes up an orbit lying within the electrodes approaches zero smoothly as Ω approaches threshold.

The trap used in the present experiments is shown schematically in Fig. 1. The disk electrodes were punched to the hyperbolic shape from a 0.175-mm tantalum sheet, and spaced at $z_0 = 25$ mm. The cylinder was formed from tantalum mesh for light transmission and high-vacuum conductance. For ease of manufacture, it was made right circular with $r_0 \approx 59$ mm, with no apparent perturbation of the ion motion. The trap was mounted in a spherical glass bulb made from a 5-liter flask. Arms were welded into the bulb for mounting a 51-mm-diam Suprasil quartz window, an electron gun, various feed throughs, and a 100-mm-diam manifold leading to a 140-liter/sec sputter-ion vacuum pump. On the manifold were mounted vacuum gauges
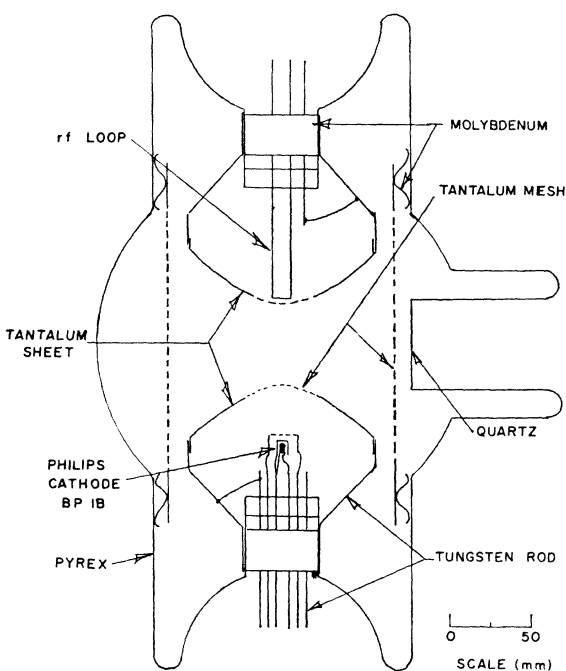
and a Kovar leak for introduction of hydrogen into the system.

After assembly, the system was evacuated with a mercury diffusion pump to about 10^{-6} Torr and baked at this pressure at temperatures up to 400°C for several days using a simple oven heated with tubular infrared lamps.[16] The system was then cooled to room temperature and sealed off, and the sputter-ion pump turned on. Within about 12 h the pressure indicated by a GF triggered discharge gauge was 3×10^{-11} Torr.

Formation of H_2^+ ions is by pulsed electron bombardment of the source gas which is maintained at an ambient pressure of 3×10^{-10} Torr by the Kovar leak. A divergent electron beam of 70-mA intensity, 800-eV average energy, and 50-msec duration is used. The pressure increases about fivefold during the bombardment.

The trapped ions may be detected by a resonance method in which their macromotion is driven by the application of a second oscillatory field at frequency ω between the disk electrodes. This second field is applied with a source with small impedance at $\omega = 0$ and $\omega = \Omega$, and is sufficiently weak that its perturbation of the ion motion is negligible except at $\omega = \omega_r$ or ω_z. In this case, the ions may be driven out of the trap.

An inductor is connected externally to the two disk electrodes forming a high-Q parallel resonant circuit tuned to a frequency near ω_z. This circuit is connected to the input of a stagger-tuned i.f. amplifier of 10^3 gain, and is made to oscillate at a peak amplitude of about 100 mV by positive feedback from the output of the amplifier through a triode limiter and a series resistance which is large compared with the shunt impedance of the tuned circuit.[17] The feedback thus approximates a constant current source. On resonance the ions effectively constitute an additional real shunt impedance, and thus cause additional damping proportional to their number. An average reading detector follows the amplifier, and its output is filtered and may be displayed on an oscilloscope.

In practice, the detector circuit is tuned to a frequency slightly above ω_z and the frequency of the ion z motion is swept through resonance by increasing ϕ_0 linearly, sweeping the oscilloscope synchronously. A block diagram of the apparatus is shown in Fig. 2, and an oscilloscope display of proton resonance in Fig. 3. The latter demonstrates the continuous creation of protons in the trap by photodissociation of the simultaneously trapped H_2^+. To trap simultaneously both H^+ and H_2^+, an emf of about 450 V peak and $\Omega/2\pi = 2$ MHz is applied to the cylinder, the disks being at rf ground potential. The axial frequency of the protons in this field is $\omega_z/2\pi \approx 300$ kHz, the depth of the proton well is $D_z \approx 12$ V, and that of H_2^+ is $D_z \approx 6$ V.

A rough estimate of the minimum number of ions

FIG. 1. Schematic drawing of ion trap.

[16] L. E. Prescott, Rev. Sci. Instr. 33, 485 (1962).
[17] A circuit of similar design for detection of nuclear resonance has been described by F. N. H. Robinson, J. Sci. Instr. 36, 481 (1959).
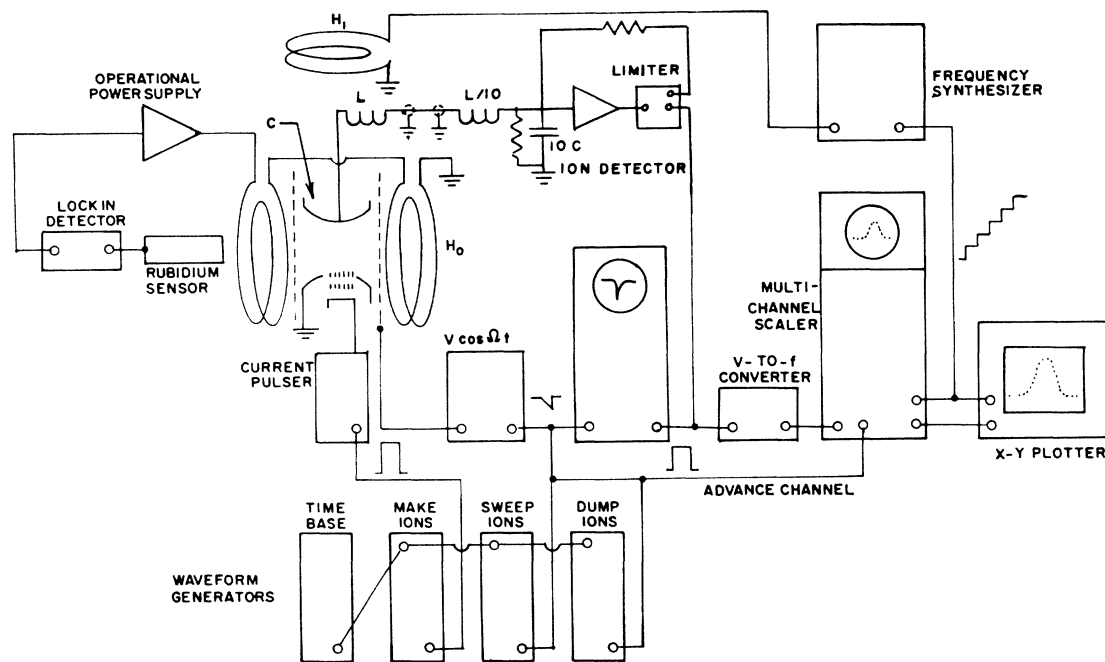
Fig. 2. Block diagram of the apparatus used for the detection of magnetic resonance in the H_2^+ molecular ion.

which can be detected by the resonance method under our operating conditions may be made. Assuming that due to unavoidable randomizing effects the ions have been distributed roughly uniformly throughout the trap volume their average binding energy will be 0.4 $eD_z \approx \frac{1}{2} eD_z$. Thus the energy required to drive out N ions is $\frac{1}{2} NeD_z$ and the average power absorbed if the well is emptied in time t_n is $NeD_z/2t_n$. For our mode of constant-current excitation, this absorption reduces the rms voltage u across the detector circuit by an amount $u_s \approx NeD_zR/2ut_n$ where R is the detector-circuit shunt resistance. The rms thermal noise voltage in the circuit in the appropriate minimum-frequency band $\approx 1/t_n$ is $u_n \approx (4RkT/t_n)^{1/2}$.

The minimum detectable ion number N_{min} is approximated by setting the voltages u_s and u_n equal. With $u \approx 0.1$ V, $R = 1$ MΩ, $D_z = 12$ V, and $t_n = 1$ msec one finds $u_n \approx 4$ μV and $N_{min} \approx 10^3$. In practice, about 5×10^6 ions were detected with a signal-to-base-line-noise ratio of 2000, or $u_s = 8$ mV, in good agreement with the ratio predicted by extrapolation from threshold.

It has been tacitly assumed here that t_n is much longer than the phase-memory times of both of the ion cloud and of the tuned circuit, as is the case in our mode of operation. In this limit, it can further be shown that u_s/u_n is independent of the choice of t_n. Treating the ion cloud as a damped harmonic oscillator in steady-state excitation, it holds that the current i_s carried by the ions is proportional to u. From an energy argument one has $i_s u t_n = $ const which, with $u_s \propto i_s$, gives $u_s^2 t_n = $ const. Since $u_n^2 t_n = $ const, the independence is shown.

PHOTODISSOCIATION

The electronic transition in H_2^+ from the $1s\sigma$ ground state to the $2p\sigma$ first excited state is followed by dissociation into a proton and ground-state hydrogen atom. The photon energy required to excite this transition depends on the vibrational state of the ion, the threshold wavelength being about $\lambda 2500$ Å for $v = 3$ and increasing roughly $\lambda 400$ Å for successive vibrational states. A recent study[18] of the relative population of the v states of H_2^+ produced by photoionization of H_2 showed good agreement with the predictions based on the Franck-Condon principle.[19] If production is by electron impact, as is the case here, the possibility of direct vibrational
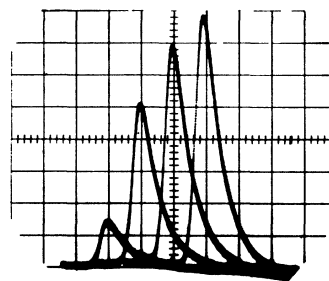

Fig. 3. Oscilloscope presentation of the detection of ions by the resonance method. Peaks represent number of H^+ ions in the trap. The production is by photodissociation of the simultaneously trapped H_2^+. The four peaks are for H^+ collection times of 50, 250, 450, and 650 msec. The largest represents 10% damping. Time base is 1 msec/division.

[18] D. C. Frost, C. A. McDowell, and D. A. Vroom, Phys. Rev. Letters **15**, 612 (1965).

[19] M. E. Wacks, J. Res. Natl. Bur. Std. **A68**, 631 (1964).
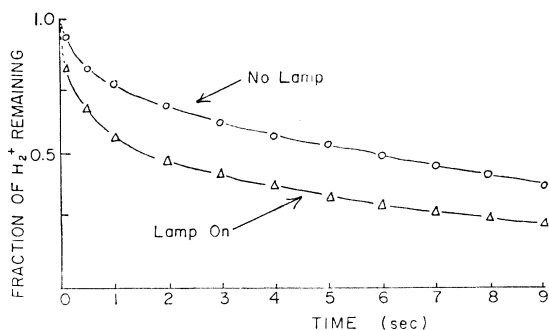
RICHARDSON, JEFFERTS, AND DEHMELT

Fig. 4. Relative number of H_2^+ ions trapped at t seconds after end of ionization pulse, for lamp on and off.

excitation or ionization from an excited state of H_2 could yield a different distribution from the above. This distribution has been measured,[20] the data suggesting a greater relative production of lower v states than predicted.

The photodissociation of H_2^+ in the present experiment is by light from a 500-W high-pressure mercury arc lamp. The manufacturer's datum shows a spectral power distribution consisting of a continuum down to $\lambda 2700$ Å plus six to eight strong lines in the visible and near ultraviolet. A parabolic front-surfaced aluminized mirror forms the beam, which is then polarized by Brewster-angle reflection from a pile of quartz plates and passed into the ion trap through the quartz window in the vacuum jacket.

The relative number of H_2^+ ions in the trap at a time t after the end of the ionizing electron pulse is shown in Fig. 4 for light on and off. The plot indicates an initial ion lifetime of about 0.2 sec in the former case and 1.6 sec in the latter. With operating parameters chosen to maximize trapping time, protons have been detected in the trap 5 min after their production. After about 2 sec the photodissociation is seen to cause negligible ion loss. By this time the ion number is about 60% of its value in the absence of light, consistent with the predicted nondissociable fraction[1] assuming the validity of the Franck-Condon principle.

ALIGNMENT

During the $1s\sigma\text{-}2p\sigma$ transition the oscillating electric dipole moment lies along the H_2^+ internuclear axis $\mathbf{k}$,[21] hence the cross section for exciting the ion to the repulsive state with linearly polarized light $\mathbf{E}$ has the orientation dependence $\cos^2(\mathbf{k},\mathbf{E})$ or $\sin^2(\mathbf{K},\mathbf{E})$, where $\hbar\mathbf{K}$ is the rotational angular momentum. Torques arising from interaction between the rotational magnetic moment and the magnetic fields, externally applied and internally generated by the nuclear and electronic spins, cause a complicated precession of $\mathbf{K}$ and time dependence of the photodissociation rate which must be

averaged. In I it was shown that light polarized parallel to an applied magnetic field is most effective in producing alignment. In sum, for this case, the depopulation of the ground state by photodissociation is described by

$$N_{FM}(t)=N_{FM}(0)\exp(-R_{FM}t/\tau), \tag{3}$$

$$R_{FM}=\tfrac{3}{2}\langle FM|\sin^2(\mathbf{K},\mathbf{H})|FM\rangle$$
$$=\tfrac{3}{2}\langle FM|(K^2-K_z^2)/K^2|FM\rangle. \tag{4}$$

Here $N_{FM}(0)$ is the initial population of the state and τ is the dissociation time, depending on the lamp intensity. The rates R_{FM} are normalized by

$$(2F+1)^{-1}\sum_{M=-F}^{M=F}R_{FM}=1. \tag{5}$$

The rates R_{FM} depend on the order of coupling of the three angular momenta, $\mathbf{K}$, $\mathbf{S}$, and $\mathbf{I}=\mathbf{I}_1+\mathbf{I}_2$, the last the sum of the two proton spins. The coupling depends in turn on the relative strengths of the magnetic interactions between pairs. Calculations by various authors, to be discussed later, indicate that the coupling between $\mathbf{I}$ and $\mathbf{S}$ is an order of magnitude greater than that between $\mathbf{K}$ and $\mathbf{S}$. Accordingly, the F_2 coupling scheme, where $\mathbf{F}_2=\mathbf{I}+\mathbf{S}$, was used in I to calculate the rates R_{FM} for the 30 magnetic sublevels of the rotational states $K=0$, 1, 2. The results, which lie between 0.500 and 1.400, were tabulated in I.

Using these results, estimates may be made of the change in ion-decay rate when substate populations are equalized by a staturating resonant rf magnetic field. An ion originally in state $|FM\rangle$ with the optical excitation rate R_{FM}/τ, is, when the resonance conditions are met, equally likely to be in each of the connected states.[22] An ensemble of ions in coupled states will then decay at a rate which is the average of those of the individual states. As a specific example, we consider the states $|KF_2FM\rangle=|1\,\tfrac{1}{2}\,\tfrac{3}{2}\,M\rangle$ for which $R_{\frac{3}{2}|\frac{3}{2}|}=0.750$ and $R_{\frac{3}{2}|\frac{1}{2}|}=1.250$. If the number of ions created in each M state is $\tfrac{1}{4}N_0$, there are, in the absence of magnetic resonance, 0.379 N_0 remaining in the four at $t=\tau$, 0.157 N_0 at $t=2\tau$, and 0.064 N_0 at $t=3\tau$, with 80% in the $|M|=\tfrac{3}{2}$ states in the last case. In a magnetic field sufficiently weak that all four M states may be connected by an rf field, the corresponding numbers are 0.368 N_0, 0.135 N_0, 0.050 N_0, all M states equally populated throughout. The percentage differences are thus 3.0, 14.6, and 24.5%. The fraction of the total ion number in resonance may be estimated. At $T=300°K$ roughly 68% of the H_2 molecules are in the $K=1$ state, the same fraction being expected for H_2^+ formed by electron bombardment.[23] It follows that 15% of the

[20] L. Kerwin, P. Marmet, and E. M. Clarke, Can. J. Phys. 39, 1240 (1961).

[21] R. S. Mulliken, J. Chem. Phys. 7, 20 (1939).

[22] Techniques such as adiabatic fast passage or 90° pulsing might in some cases be advantageous but need not be discussed here.

[23] See however, J. W. McGowan and M. A. Fineman, Phys. Rev. Letters 15, 179 (1965).

trapped ions contribute to this Zeeman multiplet, yielding a 0.45% systematic change in the H_2^+ ion number, on-resonance versus off, if it is sampled at $t=\tau$. If 10^7 ions are trapped initially and 40% are dissociable, the expected signal-to-detector-noise ratio is about 10 for this transition. The measured signal-to-noise ratio for the above Zeeman multiplet is less than unity since, in practice, the reproducibility of ion peaks is not set by the detector noise but is at best an order of magnitude less, probably because of production fluctuations. Magnetic-resonance detection requires a signal-averaging scheme, which will be described in the next section.

MAGNETIC RESONANCE

The frequencies of the transitions

$$|FF_2M\rangle \leftrightarrow |F'F_2'M'\rangle$$

in the ground state of H_2^+ range from zero up to about 1.5 GHz. The detection of each is in principle the same. As an illustrative example, the Zeeman transition discussed above will be used.

A magnetic field of between 50 mG and 1 G is applied parallel to the polarization vector of the light beam by three orthogonal pairs of Helmholtz coils of about 1-m diam. Field regulation is achieved using a rubidium optical-pumping magnetometer as a sensor which controls an error current to one pair of coils. The response time of the system is about 5 sec, with slower perturbations reduced about 50-fold.

An rf magnetic field H_1 is applied either by a coil wound around the glass bulb housing the trap, or, for the higher frequencies, a hairpin loop placed just behind the counter electrode in which small slots are cut for field penetration. The source of H_1 current in the latest version of the system is a Hewlett Packard frequency synthesizer.

The measurement cycle is as follows: with the magnetic field fixed at some value, an H_1 field is applied continuously. A 50-msec electron pulse produces H_2^+ ions. The orbiting ions are irradiated continuously by the polarized light beam. After 400-msec irradiation, the number of trapped ions is measured, as described above. For signal averaging the ion peak is applied to a voltage-to-frequency converter which yields a train of pulses, the number of which, typically 10^8, depends on the area of the ion peak. These pulses are stored in one channel of a 400-channel memory system of 10^6-counts-per-channel capacity. Following this, the ions remaining in the trap are forced out, the frequency of the H_1 field is stepped to a new value, the memory system is advanced one channel, and the cycle is repeated. After the desired frequency band is covered, the H_1 frequency and memory are reset and the scan is repeated, counts being added to those in the memory. The measurements are continued until the desired signal-to-noise ratio is obtained. The memory capacity imposes no limit since
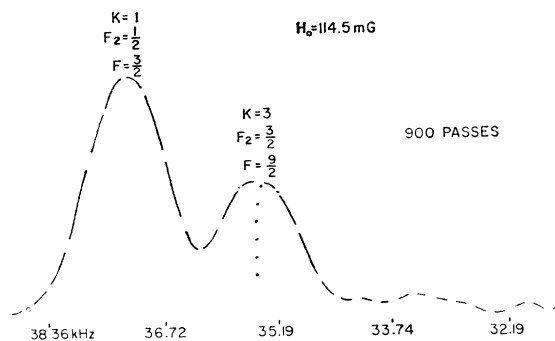

FIG. 5. Magnetic resonance in H_2^+ in a magnetic field $H_0=114.5$ mG. Peaks correspond to transitions among the Zeeman sublevels of the states shown. Integration time was 3.5 h. The locus of points under the low-frequency peak represents the centroid of a third peak, not shown, which has been replotted after all frequencies have been scaled 5/9, the theoretical value of the ratio of magnetic moments of the states $K=3$, $F=\frac{3}{2}$, and $K=1$, $F=\frac{3}{2}$.

upon overflow the count resumes at zero nondestructively. The state of the memory is monitored continuously with an oscilloscope and at the end of a measurement period a permanent record is made with an X-Y recorder. Periods of up to 15-h duration have been used in which as many as 4000 traversals are made.

The advantage this type of integration[24] has over that with the conventional lock-in detector is that by passing rapidly and repeatedly over the signal the effect of slow instrumental drift is reduced.

Figure 5 shows some of the results obtained: detection of magnetic resonance in a field of 114.5 mG. Here the number of photoproduced protons in the trap was monitored rather than the H_2^+, though either scheme yielded about the same result. An integration period of 200 min was used. The signal strength has the expected magnitude. These and similar results are discussed below.

H_2^+ SPECTRUM

Because of the two or more centers of force, molecular hyperfine interactions are more complicated than those in atoms. For the molecular hydrogens these interactions have been measured to high precision,[25] and a satisfactory explanation of the results requires an interaction Hamiltonian of some six terms.[26] Each interaction in H_2 should also be present in H_2^+, but the largest of these will be small compared with the additional interactions due to the electron paramagnetism. No complete treatment of the hyperfine interactions in H_2^+ has yet been made. However, a number of authors[27]

[24] M. P. Klein and G. W. Barton, Jr., Rev. Sci. Instr. **34**, 754 (1963).

[25] N. F. Ramsey, *Molecular Beams* (Oxford University Press, London, 1956).

[26] N. F. Ramsey, *Molecular Beams* (Oxford University Press, London, 1965), Chap. VIII.

[27] M. J. Stephen and J. P. Auffray, J. Chem. Phys. **31**, 1329 (1959); A. Dalgarno, T. N. L. Patterson, and W. B. Sommerville, Proc. Roy. Soc. (London) **A259**, 100 (1960); B. F. Burke, Astrophys. J. **132**, 514 (1960).

have calculated level splittings using the following truncated Hamiltonian:

$$H = b\mathbf{I}\cdot\mathbf{S} + cI_{z'}S_{z'} + (d_1+d_2)\mathbf{K}\cdot\mathbf{S}. \qquad (6)$$

Here $S_{z'}(I_{z'})$ is the projection of the electron (nuclear) spin on the internuclear axis. The coupling constants may be written as

$$b = g_s g_I \mu_0 \mu_N [(8\pi/3)\langle\delta(r)\rangle - \tfrac{1}{2}\langle(3z'^2-r^2)/r^5\rangle], \qquad (7)$$

$$c = \tfrac{3}{2} g_s g_I \mu_0 \mu_N \langle(3z'^2-r^2)/r^5\rangle, \qquad (8)$$

$$d_1 = 4 g_s g_K \mu_0 \mu_N \langle z'/r^3 R\rangle. \qquad (9)$$

The electron position in a coordinate system with origin at a nucleus is denoted by (z',r). The separation of nuclei is R. The angular bracket denotes averaging over electron orbit and molecular vibration and rotation. The other symbols are standard.

The constant d_2 has not been displayed. This term is a second-order contribution of significant magnitude, and arises because the molecular rotation perturbs the $^2\Sigma_g$ electronic ground state, effectively introducing some orbital angular momentum with which the electron spin interacts.[3] A knowledge of excited states of H_2^+ is necessary to calculate d_2.

The results of the various calculations of the coupling constants are summarized in Table I. All the authors have used the wave function of Bates et al.,[2] and have averaged over zero point vibration. The results are for the rotational state $K=1$, except for those of Stephen and Auffray, where they apply to $K=0$.

With these results the energy levels of the hyperfine states may be calculated. Since the coupling constant b is the largest, a first approximation to the levels is got by calculating the diagonal elements of H in the F_2 representation, which has been done by Dalgarno et al.[27] In this approximation the vector model yields the magnetic moments of the states in a weak applied field.

Mizushima[28] has calculated the levels exactly beginning with the J representation in which the third term in H has only diagonal elements, and using the coupling constants of Stephen and Auffray[27] and the assumption that $d=d_1+d_2$ is negligible. He has also calculated the magnetic moments of the states.

We have calculated the exact hyperfine levels in H_2^+ by evaluating all matrix elements in the F_2 representation, and have calculated the exact magnetic moments of the resultant mixed states. Since we wish to discuss

data such as those of Fig. 5 using this calculation, and since some of our results are in disagreement with some previously published, it seems worthwhile to include here a few details of the calculations.

The coupling of the three angular momenta may be treated in a number of ways.[29] Here we express the coupled wave function in terms of component functions:

$$|FM\rangle = \sum_{M_{F_2}M_K}\sum_{M_S M_I} C(M_S M_I, F_2 M_{F_2})$$

$$\times C(M_{F_2}M_K; FM_F)|SM_S\rangle|IM_I\rangle|KM_K\rangle. \qquad (10)$$

The C's are the Clebsch-Gordan coefficients, which are available.[30]

To use this form of the wave function it is necessary to rewrite H as a sum of products of operators which apply to component wave functions. As an example of this we consider the term $cI_{z'}S_{z'}$.

$$3cI_{z'}S_{z'} = c\mathbf{I}\cdot\mathbf{S} + c\sum_{ij} I_i S_j(3k_i k_j - \delta_{ij})$$
$$= c\mathbf{I}\cdot\mathbf{S} - [2c/(2K-1)(2K+3)]$$
$$\times\sum_{ij}\tfrac{3}{2}I_i S_j(K_i K_j + K_j K_i) - \delta_{ij}K^2. \qquad (11)$$

This procedure in which the operator, originally written in the body-centered coordinate system, has been rewritten in the laboratory system, is essentially identical to that by which a molecular electric-field gradient is transformed.[25] In its final form this term becomes[31]

$$cI_{z'}S_{z'}$$
$$= (c/3)[I_z S_z + \tfrac{1}{2}I^-S^+ + \tfrac{1}{2}I^+S^-] - (c/3)(2K-1)$$
$$\times(2K+1)[2I_z S_z(3K_z^2-K^2) - \tfrac{1}{2}(I^+S^- + S^+I^-)$$
$$\times(3K_z^2-K^2) + \tfrac{3}{2}(I_z S^- + S_z I^-)(K_z K^+ + K^+ K_z)$$
$$+\tfrac{3}{2}(I_z S^- - S_z I^-)(K_z K^+ + K^+ K_z) + \tfrac{3}{2}(I_z S^+ + S_z I^+)$$
$$\times(K_z K^- + K^- K_z) + \tfrac{3}{2}(I_z S^- + S_z I^-)(K_z K^+ + K^+ K_z)$$
$$+\tfrac{3}{2}(I_z S^+ + S_z I^+)(K_z K^- + K^- K_z) + \tfrac{1}{2}I^+S^+K^-K^-$$
$$+\tfrac{3}{2}I^-S^-K^+K^+]. \qquad (12)$$

When the other terms of H are similarly developed, all matrix elements may be obtained at once. Those of greatest immediate interest are between states formed

TABLE I. Coupling constants in the hyperfine interactions in H_2^+.

b(MHz)	c(MHz)	d_1(MHz)	d_2(MHz)	Reference[a]
880.5	128.6	−46.3	−100	A. Dalgarno et al.
890.9	132.2			M. J. Stephen and J. P. Auffray
875.74	153.51	121.50	<0.3	B. F. Burke

[a] See Ref. 27.

[28] M. Mizushima, Astrophys. J. **132**, 493 (1960).

TABLE II. Matrix elements $H_{F'F_2';FF_2}$ for the H_2^+ states with $I=1$, $S=\tfrac{1}{2}$, $K=1$.

$H_{\frac{3}{2}\frac{3}{2};\frac{3}{2}\frac{3}{2}} = b/2 + c/10 + d/2$

$H_{\frac{3}{2}\frac{3}{2};\frac{3}{2}\frac{3}{2}} = b/2 + 13c/30 - d/3$

$H_{\frac{3}{2}\frac{3}{2};\frac{3}{2}\frac{3}{2}} = b/2 - c/6 - 5d/6$

$H_{\frac{3}{2}\frac{3}{2};\frac{3}{2}\frac{3}{2}} = -b - c/3 - d/6$

$H_{\frac{3}{2}\frac{3}{2};\frac{3}{2}\frac{3}{2}} = -b - c/3 + d/3$

$H_{\frac{3}{2}\frac{3}{2};\frac{3}{2}\frac{3}{2}} = +(\sqrt{5})c/30 - (\sqrt{5})d/3$

$H_{\frac{3}{2}\frac{3}{2};\frac{3}{2}\frac{3}{2}} = -\sqrt{2}c/6 - \sqrt{2}d/3$

[29] See, for example, R. A. Frosh and H. M. Foley, Phys. Rev. **88**, 1337 (1952).

[30] J. C. Slater, Quantum Theory of Atomic Structure (McGraw-Hill Book Co., N. Y., 1960), Vol. II, p. 92.

[31] J. M. B. Kellogg, I. I. Rabi, N. F. Ramsey, and J. R. Zacharias, Phys. Rev. **57**, 677 (1940).

TABLE III. Magnetic moment ratios of some hyperfine states of H_2^+.

Ratio	Calculated	Measured	β
$g_{\frac{1}{2}-}/g_{\frac{1}{2}}$	$0.556(1+0.008+8\beta/\sqrt{5})/(1-0.004)$	$0.584(3)$	$10.4(1.3)\times10^{-3}$
$g_{\frac{1}{2}+}/g_{\frac{1}{2}}$	$1.222(1-0.003+40\beta/11\sqrt{5})/(1-0.004)$	$1.241(6)$	$8.9(3.0)\times10^{-3}$
$g_{\frac{1}{2}-}/g_{9/2}$	$1.000(1+0.008+8\beta/\sqrt{5})/(1-0.005)$	$1.051(5)$	$10.3(1.3)\times10^{-3}$

by vector coupling $I=1$, $S=\frac{1}{2}$, $K=1$ and are listed in Table II.

The off-diagonal elements in this representation are relatively small for the values of the coupling constants of Table I; hence the mixing of F_2 states is slight. However, this mixing must be considered if the measured magnetic moments are to be explained. If we designate by $|F_\pm\rangle$ the F states which are nearly pure $F_2=I\pm S$ states, the coefficients $\langle FF_2|F_\pm\rangle$ of the mixed wave functions may be written as follows:

$$\alpha=\langle\tfrac{3}{2}\tfrac{3}{2}|\tfrac{3}{2}+\rangle=-\langle\tfrac{3}{2}\tfrac{1}{2}|\tfrac{3}{2}-\rangle,$$
$$\beta=\langle\tfrac{3}{2}\tfrac{1}{2}|\tfrac{3}{2}+\rangle=\langle\tfrac{3}{2}\tfrac{3}{2}|\tfrac{3}{2}-\rangle,$$
$$\gamma=\langle\tfrac{1}{2}\tfrac{3}{2}|\tfrac{1}{2}+\rangle=-\langle\tfrac{1}{2}\tfrac{1}{2}|\tfrac{1}{2}-\rangle,$$
$$\delta=\langle\tfrac{1}{2}\tfrac{1}{2}|\tfrac{1}{2}+\rangle=\langle\tfrac{1}{2}\tfrac{3}{2}|\tfrac{1}{2}-\rangle. \tag{13}$$

Interaction of the ion with an applied magnetic field H_0 is described by

$$H=g_s\mu_0\mathbf{S}\cdot\mathbf{H}_0+g_I\mu_N\mathbf{I}\cdot\mathbf{H}_0+g_K\mu_N\mathbf{K}\cdot\mathbf{H}_0. \tag{14}$$

The electron spin contribution to the magnetic moment of each state is the following:

$$g_{\frac{3}{2}+}/g_s=\langle\tfrac{3}{2}+|S_z/M_F|\tfrac{3}{2}+\rangle,$$
$$g_{\frac{3}{2}+}/g_s=11\alpha^2/45-8\alpha\beta/9\sqrt{5}-\beta^2/9,$$
$$g_{\frac{3}{2}-}/g_s=-\alpha^2/9+8\alpha\beta/9\sqrt{5}+11\beta^2/45, \tag{15}$$
$$g_{\frac{1}{2}+}/g_s=5\gamma^2/9+8\sqrt{2}\gamma\delta/9+\delta^2/9,$$
$$g_{\frac{1}{2}-}/g_s=\gamma^2/9-8\sqrt{2}\gamma\delta/9+5\delta^2/9,$$
$$g_{\frac{3}{2}}/g_s=\tfrac{1}{5}.$$

The coefficients α and β are available from results such as those of Fig. 5 and Eq. (15). They in turn yield information on the coupling constants b, c, and d. A good first approximation to the ratios of magnetic moments of the states is got by setting $\alpha^2=1$ and $\beta=H_{\frac{1}{2}\ \frac{1}{2};\ \frac{1}{2}\ \frac{1}{2}}/H_{\frac{1}{2}\ \frac{1}{2};\ \frac{1}{2}\ \frac{1}{2}}-H_{\frac{1}{2}\ \frac{1}{2};\ \frac{1}{2}\ \frac{1}{2}}$. It is necessary to include nuclear spin and molecular rotation contributions. For this, state mixing may be ignored in first approximation. Because of possible slippage[32] the unmeasured rotational magnetic moment is not known exactly, but is here set equal to one nuclear magneton. The ratios of moments for selected states are listed in Table III, together with measured values using results such as those of Fig. 5.

The last ratio applies to the two peaks of Fig. 5,

[32] G. C. Wick, Z. Physik **85**, 25 (1933); Nuovo Cimento **10**, 118 (1933); N. F. Ramsey, Phys. Rev. **598**, 226 (1940).

the lower frequency peaks from Zeeman transitions among the sublevels of the pure state $K=3$, $F_2=\frac{3}{2}$, $F=\frac{9}{2}$. It is noteworthy that the relative magnitude of these peaks is equal to that calculated if one assumes that the relative population of the first and third rotational states of the ion is the same as that for the neutral H_2 in thermal equilibrium at $350°K$. We conclude from this that rotational excitation by the ionizing electron beam is small.

The estimated uncertainty in the measured ratios of moments is $\pm0.5\%$. The mixing coefficients calculated from these results are listed in the fourth column ($\alpha\beta<0$). Finally, the measured value of β allows one of the coupling constants to be expressed in terms of the other two. For example, using the weighted average $\langle\beta\rangle=10.1(1.6)\times10^{-3}$ we get

$$d=2.04\times10^{-2}b+11.1\times10^{-2}c. \tag{16}$$

If the calculated values of Dalgarno et al.[27] are used for b and c. we get $d=+32.2$ MHz, with an estimated uncertainty of $\pm16\%$.

One reservation should be pointed out. Because of state mixing the magnetic moments have a second-order dependence on the vibrational state of the ion. The Zeeman peaks are therefore unresolved multiplets with components from several vibrational states with $v>4$. Strictly speaking, the vibrational dependence should be considered and the measured values of β should be extrapolated to the state $v=0$ before proceeding with the analysis. However, the presently achieved precision does not warrant the greater elaboration.

TABLE IV. Energy levels of H_2^+ for the state $K=1$, $v=0$.

$E_{\frac{3}{2}+}$	486.4 MHz
$E_{\frac{3}{2}}$	469.2 MHz
$E_{\frac{1}{2}+}$	393.7 MHz
$E_{\frac{3}{2}-}$	−914.5 MHz
$E_{\frac{1}{2}-}$	−928.9 MHz

The energies of the sublevels of the state $K=1$, $v=0$ from this analysis are listed in Table IV. Transitions among these levels are more difficult to detect than those among Zeeman sublevels at low fields. Compared with the results of Fig. 5, the hyperfine signals are expected to be about ten times weaker because of vibrational and Zeeman splitting.